Thermochimica Acta 501 (2010) 24–29

Contents lists available at ScienceDirect

Thermochimica Acta

journal homepage: www.elsevier.com/locate/tca

Isothermal kinetic analysis of the thermal decomposition of kaolinite: The thermogravimetric study

Petr Ptáček[a,*], Dana Kubátová[b], Jaromír Havlica[a], Jiří Brandštetr[a], František Šoukal[a], Tomáš Opravil[a]

[a] Institute of Materials Science, Faculty of Chemistry, Brno University of Technology, Purkyňova 464/118, Brno CZ-621 00, Czech Republic
[b] Research Institute of Building Materials (VUSTAH), Hněvkovského 65, Brno CZ-617 00, Czech Republic

ARTICLE INFO

Article history:
Received 5 November 2009
Received in revised form
17 December 2009
Accepted 21 December 2009
Available online 11 January 2010

Keywords:
Kaolin
China-clay
Kaolinite
Metakaolin
Isothermal kinetics
Dehydroxylation
TGA

ABSTRACT

In this kinetic study, the dehydroxylation of the medium ordered kaolinite was investigated under isothermal conditions by the thermogravimetric analysis (TGA). The kinetic model function (mechanism) of the process and important kinetic parameters, i.e. overall activation energy (E_A) and pre-exponential (frequency) factor (A), were evaluated from the series of the thermogravimetric experiments in the temperature range from 370 to 500 °C. The linearization procedure on measured data indicates that dehydroxylation of kaolinite and metakaolinite formation up to the temperature 410 °C is controlled by the rate of the second-order chemical reaction. The overall activation energy and frequency factor of dehydroxylation were determined as 257 kJ mol^{-1} and 1.9×10^{19} s^{-1}, respectively. Above 410 °C, the course of thermal decomposition of kaolinite corresponds to a third-order reaction with the E_A value of 202 kJ mol^{-1} and 2.9×10^{15} s^{-1}, respectively.

1. Introduction

Floated kaolin is an important raw material for the ceramic technology. It is predominantly used for the production of porcelain, whereas fireclay refractory product was fabricated from crude kaolin. Beyond the ceramics, kaolin is utilized as filling agent to paper, plastics, rubber, cosmetics, etc. Metakaolin, produced by calcination of kaolin, has found utilizations in food-processing industry, oil shale processing and ceramics. Kaolinite ($Al_2Si_2O_5(OH)_4$) is the essential component of kaolin, but commonly kaolin contains a little amount of other phyllosilicates such as smectite (montmorillonite) and mica (illite) groups and tectosilicates (feldspars). The kind and amount of impurities depends on conditions of aluminosilicates (mainly feldspars) weathering. Furthermore impurities like quartz (β-SiO_2), rutile (TiO_2), hematite (Fe_2O_3) and various kinds of ferrous oxo-hydroxides may be present in kaolin too.

Kaolinite is an important dioctahedral member of kaolinite – serpetine minerals group, i.e. it belongs to phyllosilicates with 1:1 type layered structure (often designated as T–O layer). The layer consists of tetrahedral $[Si_4O_{10}]^{4-}$ and octahedral sheet (gibbsite layer), that are bound together by strong ion-covalent bond via apical oxygen. T–O layers are connected together by much weaker hydrogen bonds. Distance between two layers is about 0.72 nm. The smooth transition exists between ordered (triclinic crystal system) and disordered (triclinic-pseudomonoclinic) layered kaolinite structure. There has been also known that the smooth transition between well crystallized kaolinite and X-ray-amorphous phase with fluctuating composition between $Al_2O_3{\cdot}2SiO_2{\cdot}3H_2O$ and $Al_2O_3{\cdot}SiO_2{\cdot}2H_2O$. Kaolinite polytypes (dickite and nacrite) has been originating via alteration of aluminosilicates at higher temperature that kaolinite.

Three main thermal induced processes take place during the calcination of kaolinite. The first step is an endothermic dehydroxylation to metastable metakaolinite phase running in temperature range from 450 to 700 °C. Cubic spinel and amorphous silica are originating by exothermic reaction up to 950 °C from metakaolinite. The thermodynamically stable mullite phase is forming via exothermic reaction (Eq. (3)) over 1100 °C and crystallization of cristobalite from amorphous silica proceeds subsequently. The whole process can be mostly described by reactions [1–4]:

$$Al_2O_3 \cdot 2SiO_2 \cdot 2H_2O \xrightarrow{450-700\ ^\circ C} Al_2O_3 \cdot 2SiO_2 + 2H_2O_{(g)} \quad (1)$$

* Corresponding author. Tel.: +420 541 149 389; fax: +420 541 149 361.
E-mail addresses: ptacek@fch.vutbr.cz (P. Ptáček), kubatova@vustah.cz (D. Kubátová).

0040-6031/$ – see front matter © 2010 Elsevier B.V. All rights reserved.
doi:10.1016/j.tca.2009.12.018

$$2(Al_2O_3 \cdot 2SiO_2) \xrightarrow{925-1050\ ^\circ C} 2Al_2O_3 \cdot 3SiO_2 + SiO_2\ (amorphous) \quad (2)$$

$$3(2Al_2O_3 \cdot 3SiO_2) \xrightarrow{\geq 1050\ ^\circ C} 2(3Al_2O_3 \cdot 2SiO_2) + 5SiO_2 \quad (3)$$

$$SiO_2\ (amorphous) \xrightarrow{\geq 1200\ ^\circ C} SiO_2\ (cristobalite) \quad (4)$$

However Eqs. (1)–(4) are unable to describe the nonstoicheiometric composition of originating phases exactly. Process is also influenced by many factors, e.g. degree of disorder of the kaolinite structure [4], pressure and partial water vapour pressure [5,6], heating rate [1,6], mechanical treatments and ultrasound processing of sample [7,8]. Generally it must be influenced by the amount and kind of impurities, by particle size and degree of kaolinization.

The course of mullite formation from kaolin has been investigated by a number of methods and techniques such as molecular spectroscopy [4,5] and electron microscopy [9]. Since the Le Chatelier date the methods of thermal analysis – TGA [8,18], DTA [8], DSC [10], ETA [11] and thermodilatometry [12] stay the most applied ones.

Regardless of release of adsorbed water ($T \leq 150\ ^\circ C$), the dehydroxylation is precluded by so-called pre-dehydroxylation process that takes place in temperature range from 160 to 300 °C [11]. Dehydroxylation of kaolinite is splitting into two separate processes with T_{max} approximately at 550 and 600 °C. Water release and destruction of kaolinite sheet structure is the first one and recombination of alumina and silica to the metakaolinite structure is the second one [4].

The three basic reaction mechanisms of decomposition processes of solids are formation of a new solid phase nuclei, reaction at the product-substrate phase boundary and diffusion of gaseous products of reaction [13]. The dehydroxylation kinetics of kaolinite under isothermal conditions is mostly described by the J–M–A–Y–K (Johanson–Mehl–Avrami–Yerofeyev–Kolgomorov) equation (Eq. (5)) with the exponent n equal to 1 [6,13]. This corresponds to F_1 nucleation-growth mechanism, i.e. instantaneous nucleation and subsequent one-dimensional growth of nuclei.

$$y = 1 - \exp[-(kt)^n] \quad (5)$$

where k, t and y are overall rate constant, time and transformed phase fraction (kinetic degree of conversion), respectively. The index n, which depends on the shape of nuclei and on the dimensionality of their growth, as well as on the rate of nuclei formation, is usually known as Avrami's exponent [14,15]. Studies performed under vacuum predominantly concluded two-dimensional (D_2, Valensi equation) or three-dimensional diffusion limited process (D_3, Jander equation) [6,16,18].

Complete description of processes in heterogeneous systems is complicated due to various qualities, such as temperature, composition, particle size, nucleation sites, etc., in different part of the system. Hence the state of heterogeneous system must be described by number of parameters in addition to the temperature. These variables play the role of partial degrees of conversion. The simplification is usually made assuming a macroscopically homogeneous distribution of temperature and phase composition. Microscopic inhomogeneities are included in the model as the area of the phase boundary. The state of heterogeneous process is then expressed by the single degree of conversion (Eq. (6)) via some of property N that can be readily monitored, e.g. volume or mass. The value of y is normalized from 0 to 1 for initial ($N = N_0$) and final stage ($N = N_\infty$) of process, respectively [15].

$$y = \frac{N - N_0}{N_\infty - N_0} \quad (6)$$

The determination of activation energy and pre-exponential factor is based on logarithmic form of the Arrhenius law via plotting $\ln k$ vs. T^{-1} (Eq. (7)). The slope of this dependence is equal to $-E_A/R$. The overall activation energy of a nucleation-growth process is the sum of the partial energies of nucleation, growth and diffusion. The intercept with y-axis of Arrhenius plot is equal to the equation term $\ln A$. The value of pre-exponential factor depends on the geometry and number of sites capable to nucleation [15].

$$\ln k = \ln A - \frac{E_A}{R}\frac{1}{T} \quad (7)$$

There was published a plenty of works related to the kinetics of kaolinite dehydroxylation. With regard to influence of kaolinite structure disorder, applied method and experimental conditions is hard to reach the exact value of overall activation energy. The most frequently published values of E_A and A are placed within interval from 140 to 250 kJ mol^{-1} and from 10^8 to 10^{14} s^{-1}, respectively [6,10,13,17]. The value of activation energy is increasing with growing partial water pressure in the reaction environment and increasing of structural disorder (natural or induced by grinding) [18].

The aim of the present paper is the investigation of the kinetic mechanism and determination of pertinent kinetic parameters (overall activation energy and pre-exponential factor) of isothermal dehydroxylation of kaolinite on the basis of thermogravimetric experiments.

2. Experimental procedure

2.1. Kaolin characterization

Washed kaolin Sedlec Ia from the region Carlsbad (Czech Republic) produced by the company Sedlecký kaolin a.s. was used for this study. This high quality kaolin, originally mined in open-cast mine near village Sedlec, is commercially available since 1892 and it is often allowed to be world's standard. The content of kaolinite guaranteed by producer is higher than 90 wt.% with equivalent grain diameter median in the range 1.2–1.4 μm. The main impurities are mica group minerals and quartz. The colorant oxides content – hematite (α-Fe_2O_3) and tetragonal TiO_2 (rutile), is lower than 0.85 and 0.2 wt.%, respectively.

The 40 μm undersize was used for all following experiments and analysis. The specific surface of the sample is 20 m^2 g^{-1} (Chembet 3000). Furthermore, the initial state of the applied kaolin was investigated by the simultaneous TG-DTA (TG-DTA analyzer Q600, TA Instruments), X-ray diffraction analysis (Siemens D500) and Scanning Electron Microscopy (SEM; Tesla RS 340). Some other properties and chemical composition (determined by ICP-OES; ICP IRIS Iterdip II XSP duo) of applied kaolin are listed in Table 1.

2.2. TGA and kinetics of dehydroxylation

The course of the typical isothermal thermogravimetric experiment is shown in Fig. 1. Thermogravimetric analyses were performed with using the TG-DTA analyzer Q600 (TA Instruments). The 10 mg of sample placed in Pt crucible was heated to 110 °C (a) with rate 10 °C min^{-1} under flow of argon with rate 100 cm^3 min^{-1}. This temperature was kept for 30 min (b) to remove adsorbed water. Dry sample was then rapidly heated (100 °C min^{-1}) to desired temperature (c), which is located within investigated interval from 370 to 500 °C. Next the isothermal conditions were hold (d) for a time depending on the applied temperature (from 300 min at 500 °C to 3 days at 370 °C).

The initial stages of isothermal measurements, in which the sample attains the required temperature, are problematic and lead to uncertainty in the determination of the beginning of the reaction [15]. The mass corresponding to the initial value of the time (t_0) was used for calculation of kinetic degree of conversion according to Eq. (6). The mass of the sample at final stage (N_∞) of process

Table 1
Properties and chemical analysis of the applied kaolin Sedlec la.

Specific humidity[a]	Loos of ignition[b]	Kaolinite content[c]	Sample composition (%)[d]					
			$A1_2O_3$	SiO_2[e]	Fe_2O_3	TiO_2	CaO	MgO
0.5%	13.7%	91.8%	36.8	48.3	0.6	0.2	0,2	0,2

[a] The sample was dried at 110 °C to the reach of constant weight.
[b] The total mass loss of sample which was calcined at 1000 °C to the constant weight.
[c] The content of kaolinite was estimated from mass loss of kaolin during dehydroxylation (see Fig. 2) with regard to the theoretical value.
[d] The sample was fused with Na_2CO_3 in Pt crucible and melt was leached out by diluted HCl. The precipitated silica was filtered out and composition of the filtrate was analyzed by ICP-OES. Collected data were corrected to results of reference sample.
[e] Amount ofSiO_2 was determined by gravimetric analysis.

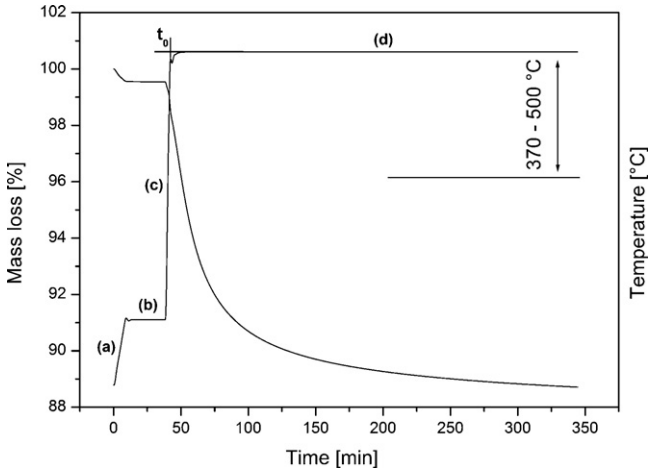

Fig. 1. (a–d) The setup of isothermal experiment and setting of the t_0 value.

was determined by non-isothermal TGA experiment (see discussion to Fig. 5). All TGA experiments were three times repeated due to elimination of the outlier results.

3. Results and discussion

3.1. Kaolin characterization

The initial state of kaolin used in this study was characterized by simultaneous TG–DTA, XRD and SEM. The typical TG–DTA plot of kaolin is shown in Fig. 2. The adsorbed water was removed below 150 °C. A small weight loss about 0.52 ± 0.08 wt.% was observed. Furthermore, there are visible two peaks on the DTA curve. The first endothermic peak at 505 ± 1 °C belongs to dehydroxylation of kaolinite according to Eq. (1). The mass of sample was reduced by about 12.82 ± 0.06 wt.% during this process. The value is getting on for the theoretical one (13.95 wt.%). That implies high content of kaolinite in applied kaolin (Table 1). The second one is a sharp exothermic peak at 985 ± 1 °C pertaining to the formation of the cubic spinel phase (Eq. (2)).

According to DTG results, the dehydroxylation of kaolinite has proceeded in the temperature interval from 315 ± 2 to 804 ± 5 °C. However, the isothermal experiments show very slow rate of reaction bellow 400 °C. Mass loss of the sample at the end of dehydroxylation interval is caused by removing of residual hydroxyl groups from the amorphous metakaolinite structure.

The XRD pattern of kaolin with labelled diffraction intensities of kaolinite and admixtures is shown in Fig. 3. Diffraction of (02, 11) band are well sensitive to the structural defects of kaolinite. Therefore, the empirical relation based on weighted peak intensity ratio can be used to estimate the degree of disorder of kaolinite [19]. The determined value of Hinckley index (HI), Aparicio–Galán–Ferrell index (AGFI) and weighted intensity ratio index (WIRI) are 1.06, 0.80 and 0.53, respectively. These values correspond to the medium-degree of structural order of applied kaolin. The identified admixture minerals in the sample are illite, quartz and smectite group minerals.

The texture of kaolin and layered kaolinite aggregate is shown in Fig. 4. The kaolinite aggregates of variable size are randomly oriented in the sample. The structure of kaolinite aggregate consists

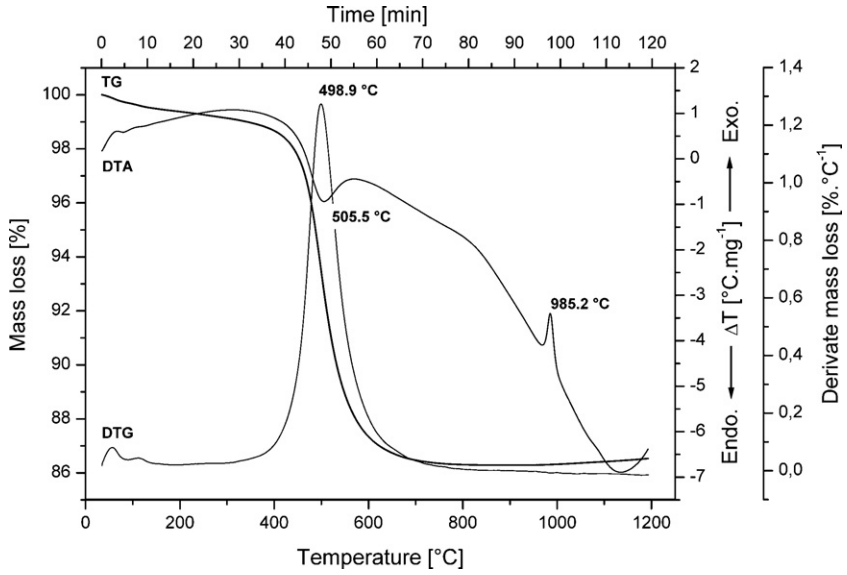

Fig. 2. Thermal analysis of kaolin. The 10 mg of sample was heated with rate 10 °C min^{-1} up to 1200 °C under flow of argon (100 cm^3 min^{-1}). The DTG curve is plotted too.

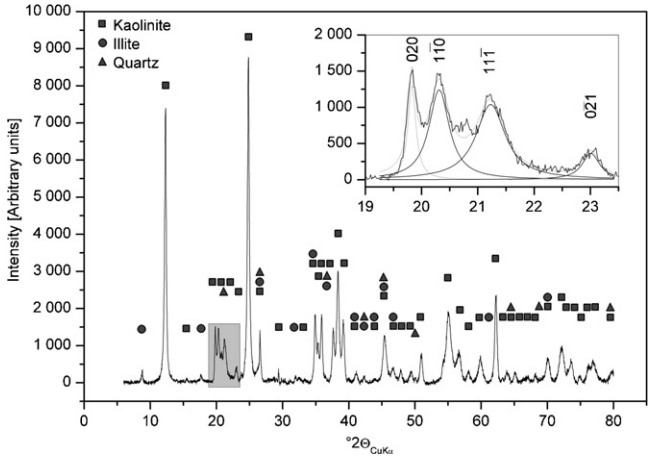

Fig. 3. Diffraction analysis of kaolin and fitting of the (02, 11) band for the determination of the structural disorder degree.

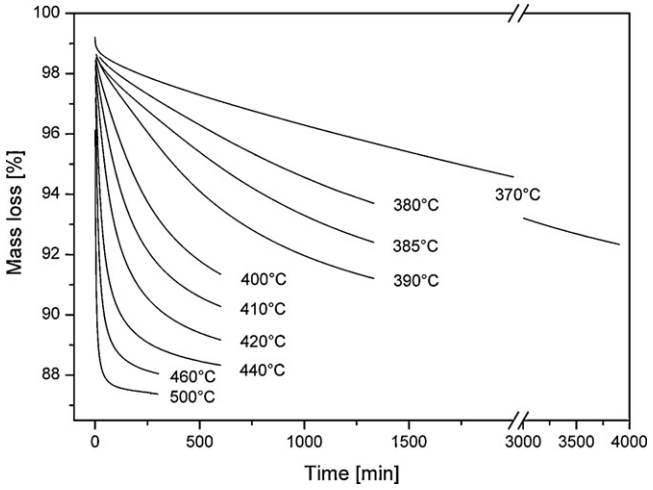

Fig. 5. Typical TGA results. Some of TG measurements are not plotted to keep lucidity of the figure.

from several columns of microscopic tabular crystal with hexagonal shape.

3.2. TGA and kinetic of dehydroxylation

The TGA curves of some isothermal experiments are shown in Fig. 5. It stands to reason that dehydroxylation is not complete even if the sample was heated at 500 °C for 5 h. The mass loss is 12.1 wt.% in this case. The reason for that is not only in insufficient time of calcination, but also in a certain content of residual hydroxyl groups which has been incorporated in the structure of metakaolin. These groups were gradually disappearing to 900–1000 °C [11].

Therefore it is difficult to obtain the same weight loss value like at non-isothermal condition in the acceptable time of experiment, especially at lower temperatures. Of course, better agreement can be reached by isothermal experiment at higher temperature, but this way have significant disadvantage too. The main part of dehydroxylation has been already carried out during heating of sample to required temperature, e.g. under undefined non-isothermal condition. With regard to above-mentioned text, the mass loss from non-isothermal assessment was taken as N_∞ value for calculation of the y value according to Eq. (6).

Determination of the most probably reaction mechanism via linearization, the procedure requires the transformation of experimentally get $y=f(t)$ dependence into $g(y)=f(t)$ function. The form of the $g(y)$ function depends on the control process of reaction, e.g. $-\ln(1-y)$ for instantaneous nucleation and one-dimensional growth of nuclei (F_1). The dependence of $g(y)$ on time must give straight line for correct kinetic (mathematical) model, because there must be fulfilled linear formula $g(y)=kt$. The proper mechanism of the process, e.g. mathematical expression of $g(y)$ function, was evaluated using mathematical models published in [13,15,20,21]. Pertinent kinetic parameters (E_A and A) were determined graphically from the Arrhenius plot.

Over investigated temperature interval, i.e. from 390 to 500 °C, the reaction mechanism has been changed. Among of all applied kinetic functions, results for the most probable and two frequently published (F_1 and D_3) mechanism are given in Table 2. The isothermal experiments carried out within temperature interval from 370 to 410 °C show the best linear fit for the reaction with the second-order kinetics (F_2).

The Arrhenius plot is shown in Fig. 6. Determined values of overall activation energy and pre-exponential factor are $257 \pm 8\,\mathrm{kJ\,mol^{-1}}$ and $1.9 \times 10^{19}\,\mathrm{s^{-1}}$, respectively.

The order of reaction was increasing (Table 2) close to temperature 410 °C and experiments carried out in temperature range

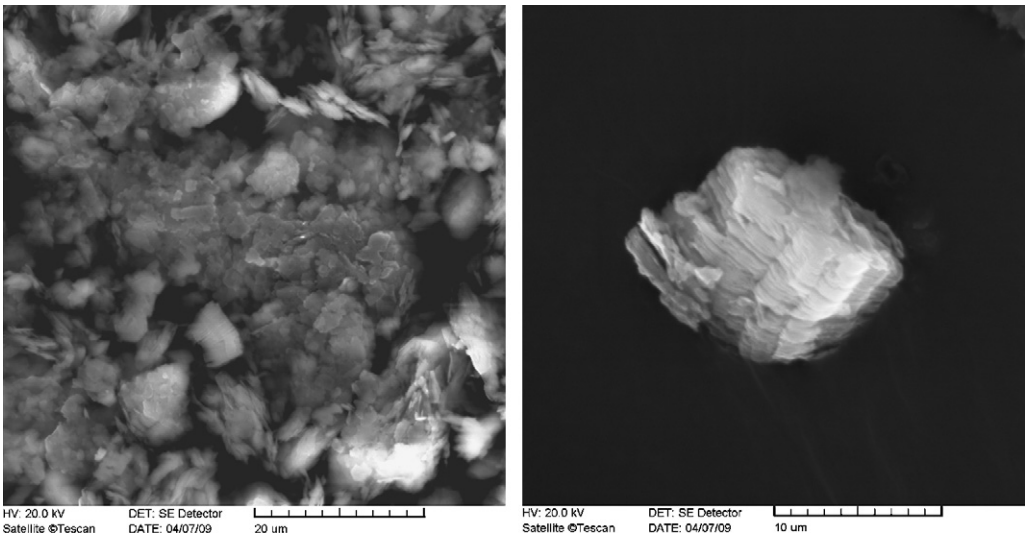

Fig. 4. Microphotograph of kaolin and kaolinite aggregate.

Table 2
Results (R^2) of linearization procedure for several isothermal experiments in the conversion range of $0.05 < y < 0.75$. In addition to the most probable mechanisms (marked by bold), results for some other frequently published kinetic function $g(y)$ are listed.

Name	Symbol	Reaction rate determining process	Kinetic model function $g(y)$	Temperature (°C)			
				370	410	415	500
Second-order eq.	F_2	Chemical reaction	$(1-y)^{-1}-1$	**0.997**	**0.994**	0.898	0.938
Third-order eq.	F_3		$(1-y)^{-2}-1$	0.970	0.993	**0.998**	**0.997**
J–M–A–Y–K eq.	F_1	Nucleation	$-\ln(1-y)$	0.974	0.937	0.472	0.573
Jander eq.	D_3	3D diffusion	$[1-(1-y)^{1/3}]^2$	0.938	0.974	0.905	0.941

from 415 to 460 °C correspond to the course of reaction of the third order (F_3). The Arrhenius plot is shown in Fig. 7. Determined values of overall activation energy and pre-exponential factor are 202 ± 3 kJ mol^{-1} and 2.9×10^{15} s^{-1}, respectively.

The determined values of overall activation energy and frequency factor were verified by the method based on the half-time of reaction ($t_{0.5}$). For $y = 0.5$, the dependence of $\ln(t_{0.5})$ on reciprocal temperature is linear with the slope equal to E_A/R [15]. The Fig. 8 pointed to that reaction mechanism was changed at temperature close to 410 °C.

Determined values of the overall activation energy and the E_A calculated from the Arrhenius plots are summarized in the Table 3. Both the methods show the good agreement of the results. That

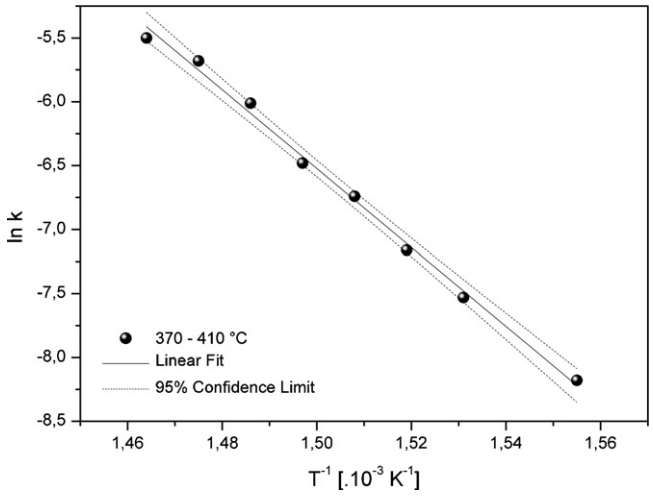

Fig. 6. The Arrhenius plot for F_2 controlled dehydroxylation of kaolinite.

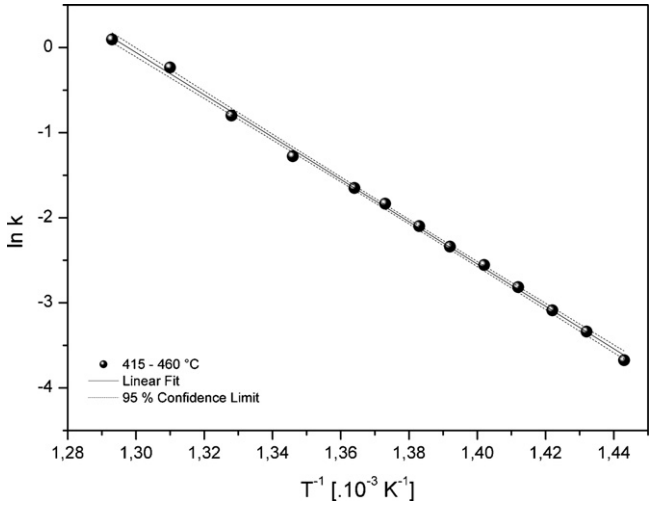

Fig. 7. The Arrhenius plot for F_3 controlled dehydroxylation of kaolinite.

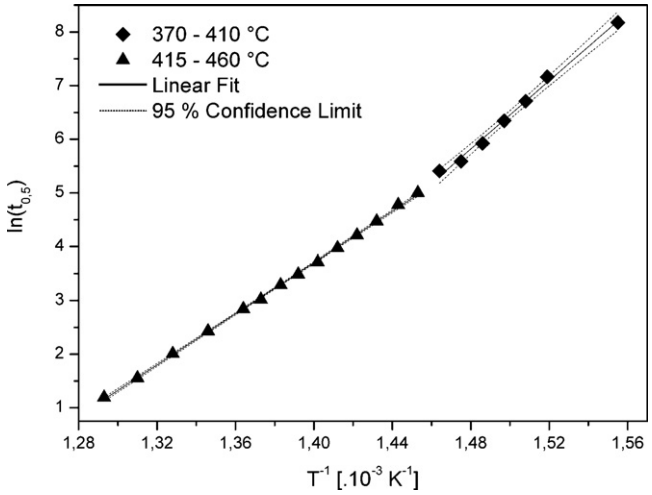

Fig. 8. The $\ln(t_{0.5})$ vs. T^1 dependence.

Table 3
Comparison of results determined by the temperature dependence of rate constant (Arrhenius law) and half-time method.

Temperature interval	370–410 °C	415–500 °C
Kinetic parameter	E_A (kJ mol^{-1})	E_A (kJ mol^{-1})
Arrhenius law	257 ± 8	202 ± 3
Half-time method	259 ± 9	198 ± 1

confirms that dehydroxylation of kaolinite has been proceeded via second-order reaction to the 410 °C and via third-order reaction at higher temperatures.

4. Conclusion

The thermal decomposition of industrial treated (washed) kaolinite is handled by the second-order reaction (F_2) in temperature interval from 370 to 410 °C. The process shows overall activation energy 257 kJ mol^{-1} and frequency factor 1.9×10^{19} s^{-1}. The reaction order increased to the third-order reaction (F_3) over the 410 °C and up to the end of studied interval (500 °C). Thereafter the dehydroxylation of kaolinite to metakaolinite shows overall activation energy 202 kJ mol^{-1} and frequency factor 2.9×10^{15} s^{-1}.

The results confirmed the finding that dehydroxylation of kaolinite is the second-order reaction [17,18,22,23]. Nevertheless, on the basis of the series of isothermal experiments it was found that reaction order changes to the third-order reaction at temperatures higher than 410 °C.

Notation

A	pre-exponential, frequency factor (s^{-1})
E_A	overall activation energy (kJ mol^{-1})
$g(y)$	function depends on the mechanism of the process
k	reaction rate constant (s^{-1})

t	time (s)
t_0	initial time of reaction (s^{-1})
$t_{0.5}$	half-time of reaction ($y = 0.5$) (s^{-1})
T	temperature (K)
N_0	initial weight of the sludge sample (mg)
N_t	weight of sludge at a given time (mg)
N_∞	weight of sludge at the completion of the process (mg)
R^2	coefficient of determination
y	fractional conversion

Acknowledgments

This paper arose out of the research projects supported by the Ministry of Education, Youth and Sports no. 1M06005 and 2B08024.

References

[1] O. Castelein, B. Soulestin, J.P. Bonnet, P. Blanchart, The influence of heating rate on the thermal behaviour and mullite formation from a kaolin raw material, Ceramics International 27 (2001) 517–522.
[2] Y.-F. Chen, M.-Ch. Wang, M.-H. Hon, Phase transformation and growth of mullite in kaolin ceramics, Journal of the European Ceramic Society 24 (2004) 2389–2397.
[3] R.L. Frost, E. Horváth, É. Makó, J. Kristóf, Á. Rédey, Slow transformation of mechanically dehydroxylated kaolinite to kaolinite—an aged mechanochemically activated formamide-intercalated kaolinite study, Thermochimica Acta 408 (2003) 103–113.
[4] K. Heide, M. Földvari, High temperature mass spectrometric gas-release studies of kaolinite $Al_2[Si_2O_5(OH)_4]$ decomposition, Thermochimica Acta 446 (2006) 106–112.
[5] J. Temuujin, K. Okada, K.J.D. MacKenzie, Ts. Jadambaa, The effect of water vapour atmospheres on the thermal transformation of kaolinite investigated by XRD, FTIR and solid state MAS NMR, Journal of the European Ceramic Society 19 (1999) 105–112.
[6] K. Nahdi, P. Llewellyn, F. Rouquérol, J. Rouquérol, N.K. Ariguib, M.T. Ayedi, Controlled rate thermal analysis of kaolinite dehydroxylation: effect of water vapour pressure on the mechanism, Thermochimica Acta 390 (2002) 123–132.
[7] C. Vizcayno, R. Castelló, I. Ranz, B. Calvo, Some physico-chemical alterations caused by mechanochemical treatments in kaolinites of different structural order, Thermochimica Acta 428 (2005) 173–183.
[8] J.L. Pérez-Rodríguez, J. Pascual, F. Franco, M.C. Jiménez de Haro, A. Duran, V. Ramírez del Valle, L.A. Pérez-Maqueda, The influence of ultrasound on the thermal behaviour of clay minerals, Journal of the European Ceramic Society 26 (2006) 74–753.
[9] H. de Souza Santos, T.W. Campos, P. de Souza Santos, P.K. Kiyohara, Thermal phase sequences in gibbsite/kaolinite clay: electron microscopy studies, Ceramics International 31 (2005) 1077–1084.
[10] K. Traoré, F. Gridi-Bennadji, P. Blanchart, Significance of kinetic theories on the recrystallization of kaolinite, Thermochimica Acta 451 (2006) 99–104.
[11] V. Balek, M. Murat, The emanation thermal analysis of kaolinite clay minerals, Thermochimica Acta 282–283 (1996) 385–397.
[12] Y.-F. Liu, X.-Q. Liu, S.-W. Tao, G.-Y. Meng, O.T. Sorensen, Kinetics of the reactive sintering of kaolinite-aluminum hydroxide extrudate, Ceramics International 22 (2002) 479–486.
[13] N. Saikia, P. Sengupta, P.K. Gogoi, P.Ch. Borthakur, Kinetics of dehydroxylation of kaolin in presence of oil field effluent treatment plant sludge, Applied Clay Science 22 (2002) 93–102.
[14] J. Farjas, P. Roura, Modification of the Kolmogorov–Johnson–Mehl–Avrani rate equation for non-isothermal experiments and its analytical solution, Acta Materialia 54 (2006) 5573–5579.
[15] J. Šesták, Thermal Analysis Part D, Volume XII D: Thermophysical Properties of Solids. Their Measurement and Theoretical Thermal Analysis (Comprehensive Analytical Chemistry), Elsevier Science (1984). ISBN-10: 0-444-99653-2.
[16] A. Ortega, F. Rouquérol, S. Akhouayri, Y. Laureiro, J. Rouquérol, Kinetical study of the thermolysis of kaolinite between −30 °C and 1000 °C by controlled rate evolved gas analysis, Applied Clay Science 8 (1993) 207–214.
[17] J.H. Levy, H.J. Hurst, Kinetics of dehydroxylation, in nitrogen and water vapour, of kaolinite and smectite from Australian Tertiary oil shales, Fuel 72 (1993) 873–877.
[18] I. Horváth, Kinetics and compensation effect in kaolinite dehydroxylation, Thermochimica Acta 85 (1985) 193–198.
[19] M. Chmielová, Z. Weiss, Determination of structural disorder degree using an XRD profile fitting procedure. Application to Czech kaolins, Applied Clay Science 22 (2002) 65–74.
[20] L. Vlaev, N. Nedelchev, K. Gyurova, M. Zagorcheva, A comparative study of non-isothermal kinetics of decomposition of calcium oxalate monohydrate, Journal of Analytical and Applied Pyrolysis 81 (2008) 253–262.
[21] Y. Duan, J. Li, X. Yang, L. Hu, Z. Wang, Y. Liu, C. Wang, Kinetic analysis on the non-isothermal dehydration by integral master-plots method and TG–FTIR study of zinc acetate dehydrate, Journal of Analytical and Applied Pyrolysis 83 (2008) 1–6.
[22] I. Horváth, G. Kranz, Y.G. Fedorenko, Entropy of activation as a possible structure-sensitive parameter in the dehydroxylation of kaolinite, Reactivity of Solids 7 (1989) 173–181.
[23] J.G. Cabrera, M. Eddleston, Kinetics of dehydroxylation and evaluation of the crystallinity of kaolinite, Thermochimica Acta 70 (1983) 237–247.